JOURNAL OF SOLID STATE CHEMISTRY **140,** 251–265 (1998)
ARTICLE NO. SC987884

# X-Ray Diffraction Study of $Cs_5(HSO_4)_3(H_2PO_4)_2$, a New Solid Acid with a Unique Hydrogen-Bond Network

Sossina M. Haile*,[1] and Pamela M. Calkins†

*Materials Science, 138-78, California Institute of Technology, Pasadena, California 91125; and †Materials Science and Engineering, University of Washington, Seattle, Washington, 98195

Received July 25, 1997; in revised form May 11, 1998; accepted May 16, 1998

**Solid solution investigations in the $CsHSO_4$–$CsH_2PO_4$ system, carried out as part of an ongoing effort to elucidate the relationship between proton conduction, hydrogen bonding, and phase transitions, yielded the new compound $Cs_5(HSO_4)_3(H_2PO_4)_2$. Single-crystal X-ray diffraction methods revealed that $Cs_5(HSO_4)_3(H_2PO_4)_2$ crystallizes in space group $C2/c$ (or possibly $Cc$), has lattice parameters $a = 34.066(19)$ Å, $b = 7.661(4)$ Å, $c = 9.158(6)$ Å, and $\beta = 90.44(6)^\circ$, a unit cell volume of 2389.9(24) Å$^3$, a density of 3.198 Mg m$^{-3}$, and four formula units in the unit cell. Sixteen non-hydrogen atoms and five hydrogen sites were located in the asymmetric unit, the latter on the basis of geometric considerations rather than from Fourier difference maps. Refinement using anisotropic temperature factors for all non-hydrogen atoms and fixed isotropic temperature factors for all hydrogen atoms yielded residuals based on $F^2$ (weighted) and $F$ values, respectively, of 0.0767 and 0.0340 for observed reflections $[F^2 > 2\sigma(F^2)]$. The structure contains layers of $(CsH_2XO_4)_2$ that alternate with layers of $(CsHXO_4)_3$, where $X$ is P or S. The arrangement of Cs, H, and $XO_4$ groups within the two types of layers is almost identical to that in the end-member compounds, $CsH_2PO_4$ and $CsHSO_4$-II, respectively. Although P and S each reside on two of the three $X$ atom sites in $Cs_5(HSO_4)_3(H_2PO_4)_2$, the number of protons in the structure appears fixed. In addition, the correlation of S–O and S–OH bond distances with O···O distances, where the latter represents the distance between two hydrogen-bonded oxygen atoms, was determined from a review of literature data.**


## INTRODUCTION

Proton transport in hydrogen-bonded systems has intrigued scientists since Bjerum (1) first identified "L" and "D" defects in ice as the species by which proton motion occurs. More recently, solid acid sulfates and selenates, such as $CsHSO_4$ (2), $Rb_3H(SeO_4)_2$ (3), and $Cs_5H_3(SeO_4)_4 \cdot xH_2O$ (4) and their deuterated analogs, have come under intense investigation. Over the past 15 years almost 50 experimental papers have appeared on $CsHSO_4$ alone, covering such topics as X-ray and neutron structure determination, AC impedance spectroscopy, quasielastic neutron scattering, incoherent neutron scattering, polarized Raman and IR single-crystal spectroscopy, calorimetry, decomposition, high pressure investigations, pulsed field gradient NMR, acoustic wave propagation, etc. These materials are of interest because each undergoes a structural transition at elevated temperatures, at which point the conductivity jumps by as much as 5 orders of magnitude. Despite the number and variety of experiments that have been carried out on solid acid sulfates and selenates, no generally agreed upon model describing the chemical and structural features that induce superprotonic phase transitions exists. Indeed, until our recent investigations of the $CsHSO_4$–$CsH_2PO_4$ system and the discovery of superprotonic behavior in $\alpha$-$Cs_3(HSO_4)_2(H_2PO_4)$ (5), it was not known with certainty whether phosphate containing compounds could also undergo such transitions.

The present investigations in the $CsHSO_4$–$CsH_2PO_4$ system have been undertaken in order to elucidate the relationship between proton conduction, hydrogen bonding and phase transitions. Specifically, we hoped to determine the impact of such crystal chemical features as the dimensionality of the hydrogen-bonded network, the geometry of locally disordered hydrogen bonds, and the presence of proton "interstitials" and/or "vacancies" on the superprotonic transition and the magnitude of proton conductivity. As stated in (6), this particular system is ideal for such a study because (i) $CsHSO_4$ is a well-characterized material with a superprotonic transition at 141°C (2); (ii) the chemical similarity between S and P and the structural similarity between $CsHSO_4$ and $CsH_2PO_4$ (at room temperature (7, 8)) suggests that any compound within this system, including the end-members, should exist over a significant composition range, and hence the proton content should be subject to control via control of the stoichiometry; and

[1] To whom correspondence should be addressed.



0022-4596/98 $25.00

(iii) the fact that $CsHSO_4$ and $CsH_2PO_4$ are, despite their similarities, not isostructural precludes complete solid solubility and suggests that new intermediate compounds should exist. In this case, control of the $H:XO_4$ ratio provides control of the overall hydrogen-bonding scheme.

From our first studies of $\alpha$-$Cs_3(HSO_4)_2(H_2PO_4)$ (5), and more recently of $\beta$-$Cs_3(HSO_4)_2(H_{2-x}(P_{1-x}S_x)O_4)$ (6), both of which undergo superprotonic phase transitions, we not only concluded that phosphorus does not inhibit superprotonic behavior but also proposed that the presence of oxygen atoms with different hydrogen-bond environments, at room temperature, is a key prerequisite for superprotonic behavior at elevated temperatures. When such a nonuniform hydrogen-bond network exists, entropic considerations, which favor chemically equivalent bonds, drive a transition to a disordered state, and it is precisely this disorder that leads to superprotonic conductivity. In the present work, we describe the structure of $Cs_5(HSO_4)_3(H_2PO_4)_2$, the newest member of the sulfate–phosphate class of hydrogen-bonded compounds, and provide a comparison of its structure to that of others in this family. In addition, we offer some predictions about its physical properties on the basis of this structure determination.

## EXPERIMENTAL

### *Crystal Growth and Composition Determination*

Crystals of $Cs_5(HSO_4)_3(H_2PO_4)_2$ were grown from aqueous solutions containing $Cs_2CO_3$, $H_2SO_4$, and $H_3PO_4$ in which the molar ratio of Cs : S : P was 1 : 0.5 : 0.5. Slow evaporation of water under ambient conditions over a period of several days yielded small crystals of multiple phases, from which the title compound was extracted. Other phases obtained were $\alpha$-$Cs_3(HSO_4)_2(H_2PO_4)$, $Cs_2SO_4$, and, on occasion, $CsH_5(PO_4)_2$, and these, in fact, comprised the bulk of the precipitate. Preparation of crystalline powder by rapid precipitation from similar solutions (where the precipitation was induced by the introduction of acetone) resulted in the synthesis of a new compound that remains to be identified.

The composition of crystals obtained from the slow evaporation (and identified as the desired phase on the basis of single crystal lattice constant measurements) was determined by energy dispersive spectroscopy (electron microprobe). Samples were mounted in an epoxy resin, polished, and then sputter-coated with gold to obtain a conductive surface. Characteristic peak intensities were measured with a JEOL Superprobe 733 and converted into mass percent using Tracor Northern analytical software (9). The compounds $CsHSO_4$, $CsH_2PO_4$, and $\alpha$-$Cs_3(HSO_4)_2(H_2PO_4)$ served as standards.

The microprobe data, collected from two separate crystals, at four and five positions, respectively, indicated that the mole ratio of Cs : (P + S) was 1.04(3) and that of S : P was 1.3(2). Both values are within two standard deviations of the ideal values of 1 and 1.5, respectively, for a compound of composition $Cs_5(HSO_4)_3(H_2PO_4)_2$. The observed molar ratios of S : P ranged from a low of 1.01 to a high of 1.64, and this large variation was attributed to the use of an EDS rather than WDS (wavelength dispersive spectroscopy) system. Attempts to measure compositions by the latter technique were unsuccessful as the long count times induced crystal damage.

### *Intensity Data Collection and Structure Determination*

Single-crystal X-ray intensity data were collected at room temperature from an as-synthesized specimen measuring $0.2 \times 0.2 \times 0.2$ mm$^3$. Data were obtained in Mo$K\alpha$ radiation ($\lambda = 0.71073$ Å) using a Crystal Logic four-circle diffractometer. Refinement of the lattice parameters, using the locations of 25 peaks, revealed $Cs_5(HSO_4)_3(H_2PO_4)_2$ to be $C$-centered monoclinic with lattice parameters $a = 34.066(19)$ Å, $b = 7.661(4)$ Å, $c = 9.158(6)$ Å, and $\beta = 90.44(6)^\circ$. The remaining data collection parameters, along with relevant crystallographic data and parameters related to the refinement, are provided in Table 1.

Analysis of the systematic absences indicated a diffraction symbol of $C^*c^*$, permitting space groups $C2/c$ and $Cc$. The centric, $C2/c$, was selected as the starting point for the solution of the structure. The Cs and $X$ atom sites, where $X$ = P or S, were located from direct methods, and the O atom sites from subsequent Fourier difference maps. Phosphorus and sulfur atom sites were distinguished on the basis of crystal-chemical considerations, as discussed below. Such considerations also enabled identification of hydrogen positions. In the final cycles of the refinement a single fixed, isotropic displacement parameter was employed for hydrogen atoms and (refined) anisotropic displacement parameters for all other atoms. In addition, an extinction correction parameter was incorporated into the refinement. It became apparent, however, that the correction could not adequately describe the reduction in intensity of very strong peaks and, thus, those peaks of intensity greater than 15,000 cps (188 of 2343 collected reflections) were omitted from the final refinement.

The final residuals were 0.0917 (weighted) and 0.0487, as calculated for $F^2$ and $F$, respectively, using all data. Analogous residuals determined from observed data [$F^2 > 2\sigma(F^2)$] were 0.0767 and 0.0340. Refinement was carried out by minimizing a weighted residual based on $F^2$ using all data (as per the SHELXL (12) program); the value of $R(F)$, a residual based on $F$ values, is provided only for comparison with literature $R$ values, typically derived from refinements on $F$. Calculated and observed $F^2$ have been

**TABLE 1**
**Crystal Data, Data Collection Parameters, Data Refinement Parameters, and Other Experimental Details for the Structure Determination and Refinement of $Cs_5(HSO_4)_3(H_2PO_4)_2$**

| | |
|---|---|
| **Crystal data** | |
| Temperature | 293(2) K |
| Compound name | $Cs_5(HSO_4)_3(H_2PO_4)_2$ |
| Formula | $Cs_5S_3P_2O_{20}H_7$ |
| Crystal system | Monoclinic |
| Space group | $C2/c$ |
| Unit cell dimensions | $a = 34.066(19)$ Å<br>$b = 7.661(4)$ Å<br>$c = 9.158(6)$ Å<br>$\beta = 90.44(6)^\circ$ |
| Unit cell volume | 2389.9(24) Å$^3$ |
| Formula weight | 1150.74 au |
| Z | 4 |
| Density (calculated) | 3.198 Mg m$^{-3}$ |
| Absorption coefficient | 8.029 mm$^{-1}$ |
| Crystal size | $0.20 \times 0.20 \times 0.20$ mm$^3$ |
| Crystal shape | Cube |
| Crystal color | Colorless |
| Crystal mounted | On glass fiber with epoxy |
| No. of reflections for cell measurement | 25 ($5.1 < \theta < 10.1^\circ$) |
| **Data collection** | |
| Radiation | X-ray, Mo$K\alpha$ |
| Wavelength | 0.71073 Å |
| Instrument | Crystal Logic Diffractometer |
| Data collection method | $\theta$–$2\theta$ scan |
| F(000) | 2080 |
| Absorption correction method | Empirical, $\psi$ scan |
| Maximum and minimum transmission factors | 0.87 and 1.00 |
| $\theta$ range for data collection | 1.2–22.5° |
| Index ranges | $0 \le h \le 23$, $-8 \le k \le 8$, $-11 \le l \le 9$ |
| No. of reflections collected | 2155 |
| No. of independent reflections | 1098 [$R$(int) = 0.0249] |
| No. of significant reflections | 959 [$I \ge 2\sigma$] |
| Standards | [(10, 0, 0), (−6, 0, 2), (4, 0, −2)] |
| Deviation of standards from initial value | −2.9% |
| Decay correction | Applied |
| **Refinement** | |
| Refinement method | $F^2$ |
| w$R$ [$F^2 > 2\sigma(F^2)$] | 0.0767 |
| w$R(F^2)$ | 0.0917 |
| $R$ [$F > 4\sigma(F)$] | 0.0340 |
| Goodness-of-fit, $S$, on $F^2$ | 1.335 |
| No. of reflections used in refinement | 1098 |
| No. of refined parameters | 144 |
| Weighting scheme | $w = [\sigma^2(F_o^2) + (0.0374*P)^2]^{-1}$, where $P = (1/3)*(\mathrm{Max}(F_o^2, 0) + 2*F_c^2)$ |
| $(\Delta/\sigma)$, max/mean | 0.000, 0.000 |
| Fourier difference peaks, max/min | 1.634/−1.706 e A$^{-3}$ |
| Anisotropic thermal parameters | All non-hydrogen atoms |
| Extinction coefficient | 0.0030(2) |
| Sources of atomic scattering factors | Cromer and Waber (10) |
| Treatment of H atom | Constrained refinement (see text) |
| **Computer programs** | |
| Structure solution | SHELXS (11) |
| Structure refinement | SHELXL (12) |
| Structure depiction | ATOMS from Shape Software |

**TABLE 2**
**Atomic Coordinates and Equivalent Isotropic Displacement Parameters for $Cs_5(HSO_4)_3(H_2PO_4)_2$[a]**

| Atom | Site | $x$ | $y$ | $z$ | $U_{eq}$ |
|---|---|---|---|---|---|
| Cs(1) | 4$e$ | $\frac{1}{2}$ | 0.08511(13) | $\frac{1}{4}$ | 0.0456(5) |
| Cs(2) | 8$f$ | 0.18691(3) | 0.49508(11) | 0.24579(9) | 0.0572(5) |
| Cs(3) | 8$f$ | 0.09824(3) | 0.13850(9) | 0.95988(9) | 0.0456(5) |
| P(1)* | 4$e$ | $\frac{1}{2}$ | 0.5881(5) | $\frac{1}{4}$ | 0.0289(13) |
| S(1)** | 4$e$ | $\frac{1}{2}$ | 0.5881(5) | $\frac{1}{4}$ | 0.0289(13) |
| P(2)* | 8$f$ | 0.20945(12) | −0.0059(4) | 0.4895(3) | 0.0400(12) |
| S(2)** | 8$f$ | 0.20945(12) | −0.0059(4) | 0.4895(3) | 0.0400(12) |
| S(3) | 8$f$ | 0.40554(12) | 0.8696(4) | 0.0046(3) | 0.0380(11) |
| $O(1)_A$ | 8$f$ | 0.4658(2) | 0.6956(10) | 0.2970(8) | 0.041(2) |
| $O(2)_{A/D}$ | 8$f$ | 0.4874(3) | 0.4679(9) | 0.1259(8) | 0.041(2) |
| $O(3)_{A/D}$ | 8$f$ | 0.2149(3) | 0.1874(11) | 0.4836(11) | 0.068(3) |
| $O(4)_{A/D}$ | 8$f$ | 0.2490(3) | 0.9116(11) | 0.5090(13) | 0.067(3) |
| $O(5)_A$ | 8$f$ | 0.1883(3) | 0.9226(14) | 0.3579(9) | 0.075(3) |
| $O(6)_D$ | 8$f$ | 0.1829(3) | 0.9375(14) | 0.6141(9) | 0.074(3) |
| O(7) | 8$f$ | 0.4059(3) | 0.7446(11) | 0.8877(9) | 0.067(3) |
| O(8) | 8$f$ | 0.3710(3) | 0.9779(11) | 0.0029(10) | 0.054(3) |
| O(9) | 8$f$ | 0.4413(3) | 0.9723(11) | 0.0134(10) | 0.052(3) |
| $O(10)_D$ | 8$f$ | 0.4025(3) | 0.7633(11) | 0.1519(9) | 0.054(3) |
| H(1) | 4$d$ | $\frac{1}{4}$ | $\frac{1}{4}$ | $\frac{1}{2}$ | 0.080 |
| H(2) | 8$f$ | 0.4302(21) | 0.7385(178) | 0.1897(136) | 0.080 |
| H(3) | 4$a$ | $\frac{1}{2}$ | $\frac{1}{2}$ | 0 | 0.080 |
| H(4) | 4$c$ | $\frac{1}{4}$ | $\frac{3}{4}$ | $\frac{1}{2}$ | 0.080 |
| H(5) | 8$f$ | 0.1856(40) | 0.9988(147) | 0.7342(75) | 0.080 |

* Occupancy fixed at $\frac{2}{3}$.
** Occupancy fixed at $\frac{1}{3}$.
[a] The term $U_{eq}$ is defined as one third of the trace of the orthogonalized $U_{ij}$ tensor. Numbers in parentheses indicate esd in last digit(s). Subscripts A, D, and A/D denote oxygen acceptor, donor, and mixed acceptor/donor atoms, respectively.

deposited.[2] The atomic coordinates and thermal parameters obtained are given in Tables 2 and 3, respectively. Interatomic distances in the cation coordination polyhedra are reported in Table 4. For sulfate and phosphate groups, interatomic angles are also reported.

From the X-ray data alone, it was not possible to directly determine which of the $X$ atoms should be sulfur and which should be phosphorus. However, on the basis of the average $X$–O distances, it was concluded that the $X$ atom at the second 8$f$ site ($\langle d_{X-O} \rangle = 1.477$ Å, Table 3) must consist entirely of sulfur. The average $X$–O distance at the other two $XO_4$ group sites are both 1.508 Å, suggesting that both

[2] See NAPs document No. 05480 for 7 pages of supplementary material. Order from ASIS/NAPS Microfiche Publications, P.O. Box 3513, Grand Central Station, New York, NY 10163. Remit in advance $4.00 for microfiche copy or for photocopy, $7.75 up to 20 pages plus $0.30 for each additional page. All orders must be prepaid. Institutions and Organizations may order by purchase order. However, there is a billing and handling charge for this service of $15. Foreign orders add $4.50 for postage and handling, for the first 20 pages, and $1.00 for additional 10 pages of material, $1.50 for postage of any microfiche orders.

**TABLE 3**
**Anisotropic Displacement Parameters for $Cs_5(HSO_4)_3(H_2PO_4)_2$[a]**

| Atom | $U_{11}$ | $U_{22}$ | $U_{33}$ | $U_{23}$ | $U_{13}$ | $U_{12}$ |
|---|---|---|---|---|---|---|
| Cs(1) | 0.0453(12) | 0.0342(6) | 0.0571(8) | 0 | −0.0043(7) | 0 |
| Cs(2) | 0.0528(11) | 0.0783(7) | 0.0405(6) | −0.0030(4) | −0.0018(5) | 0.0000(5) |
| Cs(3) | 0.0366(10) | 0.0358(5) | 0.0644(6) | 0.0022(4) | 0.0013(5) | −0.0013(4) |
| P(1) | 0.032(4) | 0.034(2) | 0.021(2) | 0 | −0.001(2) | 0 |
| S(1) | 0.032(4) | 0.034(2) | 0.021(2) | 0 | −0.001(2) | 0 |
| P(2) | 0.037(4) | 0.049(2) | 0.034(2) | 0.0011(14) | 0.001(2) | −0.005(2) |
| S(2) | 0.037(4) | 0.049(2) | 0.034(2) | 0.0011(14) | 0.001(2) | −0.005(2) |
| S(3) | 0.043(3) | 0.034(2) | 0.037(2) | −0.0015(12) | −0.004(2) | 0.001(2) |
| $O(1)_A$ | 0.036(7) | 0.046(5) | 0.041(5) | 0.009(4) | 0.005(4) | 0.014(4) |
| $O(2)_{A/D}$ | 0.054(7) | 0.045(4) | 0.024(4) | −0.007(3) | −0.004(4) | −0.019(4) |
| $O(3)_{A/D}$ | 0.055(8) | 0.037(5) | 0.111(8) | 0.008(5) | −0.010(6) | −0.003(5) |
| $O(4)_{A/D}$ | 0.026(8) | 0.037(5) | 0.138(9) | −0.010(5) | −0.009(6) | −0.005(5) |
| $O(5)_A$ | 0.098(9) | 0.093(7) | 0.033(5) | 0.005(5) | −0.014(6) | −0.037(7) |
| $O(6)_D$ | 0.089(10) | 0.093(7) | 0.039(5) | −0.010(5) | 0.009(5) | −0.037(7) |
| O(7) | 0.105(9) | 0.044(5) | 0.052(5) | −0.014(4) | 0.002(5) | −0.001(5) |
| O(8) | 0.033(9) | 0.054(5) | 0.074(7) | 0.011(4) | −0.004(5) | 0.014(5) |
| O(9) | 0.033(9) | 0.060(6) | 0.064(6) | 0.009(4) | 0.004(5) | −0.007(5) |
| $O(10)_D$ | 0.053(8) | 0.062(5) | 0.046(5) | 0.014(4) | −0.001(5) | 0.007(5) |

[a] The anisotropic displacement factor exponent takes the form $-2\pi^2[h^2a^{*2}U_{11} + \cdots + 2hka^*b^*U_{12} + \cdots]$. Numbers in parentheses indicate esd in last digit(s).

S and P occupy both sites. The chemical analysis, as indicated above, yielded approximate atomic ratios of Cs : S : P of 5 : 3 : 2, and thus it was presumed that both the 4*e* site and the remaining 8*f* site were occupied by $\frac{2}{3}$P and $\frac{1}{3}$S.

These conclusions about the appropriateness of *X* atom sites to either P or S on the basis of *X*–O bond length considerations can be more quantitatively arrived at by an examination of the bond valence sums at these sites. Because of the chemical similarity of phosphorus and sulfur, the bond valence contributions of S–O and P–O bonds are virtually identical, given respectively by

$$S(\text{P–O}) = \exp[(1.617 - d_{\text{P–O}})/0.37] \qquad [1]$$

and

$$S(\text{S–O}) = \exp[(1.624 - d_{\text{S–O}})/0.37], \qquad [2]$$

where $d_{\text{P–O}}$ and $d_{\text{S–O}}$ are the phosphorous-to-oxygen and sulfur-to-oxygen bond distances, respectively, measured in Å (13). Thus, one need not accurately assign occupancies at the *X* atom sites in order to determine the sum of the bond valences. Taking the 4*e* and the first 8*f* site to be occupied by both S and P, as described above, the sum of the bond valences are 5.42 and 5.46, respectively, which are consistent with the presumed occupancies. Similarly, the sum of the bond valences at the second 8*f* site is 6.02, and in good agreement with the assumption of full occupancy by sulfur.

Whenever one observes a random distribution of two atomic species on the same site, as appears to be the case here, one must consider the possibility of ordering such that a superstructure is formed. In the present structure, one might anticipate a tripling of the one of the lattice constants with the P and S atoms taking up ordered arrangements on the 4*e* and first 8*f* sites. Although a concerted effort to find such superstructure peaks was not made at the time of data collection, no such reflections appeared in the initial stage of unit cell determination. In any case, the similarity of the scattering lengths of $P^{5+}$ and $S^{6+}$ would render such reflections very weak and quite likely unobservable by X-ray methods.

With the distribution of sulfur and phosphorous established, the next step in the structure determination was the identification of hydrogen atom positions. An examination of intertetrahedra oxygen–oxygen distances suggested that five hydrogen sites existed, three of which linked oxygen atoms related by inversion symmetry and two of which linked crystallographically distinct oxygen atoms (Table 5). The assumption that protons fully occupy each of these sites provides for a total of seven protons per formula unit and yields a stoichiometry that is consistent with the chemical analysis. It was then noted that of the two $XO_4$ groups residing at 8*f* sites, the latter has only one oxygen atom that participates in hydrogen bonds (as compared to all 4 for the first 8*f* $XO_4$ group), which is consistent with its assignment as a sulfate anion. Peak positions in the Fourier difference map at approximately the correct location with respect to the oxygen atoms were used as initial protons coordinates. Specifically, where the proton linked two crystallographically independent oxygen atoms, H(2) and H(5), a peak at $\sim$1 Å from the donor oxygen atom was taken to represent the proton; donor, $O_D$, and acceptor, $O_A$, oxygen atoms were distinguished on the basis of *X*–O bond lengths, with longer distances being associated with donors and shorter distances with acceptors. The positions of the H(2) and H(5) protons were refined under the restraint that the $O_D$–H distances be 1.02(5) and 1.19(5), respectively. These values were selected on the basis of the correlation obtained by Ichikawa (15) between O ⋯ O distances and O–H distances. In the case of H(1), H(3), and H(4), where the proton linked two oxygen atoms related by a center of symmetry, attempts to refine a model in which the proton was given $\frac{1}{2}$ occupancy at a position just off the symmetry element were attempted, but proved unsuccessful in that unrealistic bonding geometries were obtained. Therefore, these atoms were placed directly on the center of symmetry in the final refinement in space group $C2/c$, and the oxygen atoms to they are bonded are referred to as mixed acceptor/donors, $O_{A/D}$. It is noteworthy that refinement of a model that excluded protons and assumed a uniform distribution of P and S atoms at the three *X* atom sites yielded a residual of 0.0969. In comparison, the introduction of protons (at the positions given in Table 2) and the assumption of ordering of P and S atoms reduced w$R(F^2)$ to 0.0917, as given in Table 1. It is also noteworthy that the O ⋯ O distances between

**TABLE 4**
**Coordination Polyhedra in $Cs_5(HSO_4)_3(H_2PO_4)_2$ (Numbers in Parentheses Indicate esd in Last Digit(s))**

(a) Interatomic distances (Å) in the cesium polyhedra; sum of the bond valences at Cs also given

| | | | | | |
|---|---|---|---|---|---|
| Cs(1)–O(9) | 3.062(10) | Cs(2)–O(8) | 3.008(10) | Cs(3)–O(2) | 3.122(9) |
| Cs(1)–O(9) | 3.062(10) | Cs(2)–O(8) | 3.045(10) | Cs(3)–O(8) | 3.138(9) |
| Cs(1)–O(2) | 3.173(8) | Cs(2)–O(4) | 3.200(11) | Cs(3)–O(1) | 3.160(7) |
| Cs(1)–O(2) | 3.173(8) | Cs(2)–O(4) | 3.270(12) | Cs(3)–O(10) | 3.244(9) |
| Cs(1)–O(9) | 3.175(9) | Cs(2)–O(3) | 3.343(9) | Cs(3)–O(5) | 3.248(11) |
| Cs(1)–O(9) | 3.175(9) | Cs(2)–O(5) | 3.432(11) | Cs(3)–O(7) | 3.253(9) |
| Cs(1)–O(1) | 3.234(8) | Cs(2)–O(6) | 3.529(11) | Cs(3)–O(6) | 3.255(11) |
| Cs(1)–O(1) | 3.234(8) | Cs(2)–O(3) | 3.554(10) | Cs(3)–O(9) | 3.282(9) |
| Cs(1)–O(7) | 3.693(10) | Cs(2)–O(10) | 3.653(9) | Cs(3)–O(7) | 3.287(8) |
| Cs(1)–O(7) | 3.693(10) | Cs(2)–O(7) | 3.925(10)* | Cs(3)–O(10) | 3.682(8) |
| $\sum S = 1.15$ | $\langle 3.27 \rangle$ | $\sum S = 0.90$ | $\langle 3.34 \rangle$ | $\sum S = 1.07$ | $\langle 3.27 \rangle$ |

(b) Interatomic distances (Å) and angles (deg) in phosphorus and sulfur tetrahedra; sum of the bond valences at P and S sites also given

| | Distance | Angle | Distance | Angle | Distance | Angle | Distance |
|---|---|---|---|---|---|---|---|
| P(1)/S(1) | | | | | | | |
| $O(1)_A$ | 1.493(8) | | | | | | |
| $O(1)_A$ | 1.493(8) | 113.0(7) | 2.490(15) | | | | |
| $O(2)_{A/D}$ | 1.522(8) | 109.6(4) | 2.463(11) | 109.4(5) | 2.460(11) | | |
| $O(2)_{A/D}$ | 1.522(8) | 109.4(5) | 2.460(11) | 109.6(4) | 2.463(11) | 105.6(6) | 2.424(15) |
| $\sum S = 5.42$ | $\langle 1.508 \rangle$ | O(1) | O(1) | O(1) | O(1) | O(2) | O(2) |
| P(2)/S(2) | | | | | | | |
| $O(3)_{A/D}$ | 1.493(9) | | | | | | |
| $O(4)_{A/D}$ | 1.499(10) | 108.0(5) | 2.421(12) | | | | |
| $O(5)_A$ | 1.503(10) | 113.1(6) | 2.500(13) | 111.5(7) | 2.481(15) | | |
| $O(6)_D$ | 1.523(10) | 112.6(6) | 2.510(13) | 109.2(7) | 2.463(14) | 102.3(6) | 2.358(12) |
| $\sum S = 5.46$ | $\langle 1.508 \rangle$ | O(3) | O(3) | O(4) | O(4) | O(5) | O(5) |
| S(3) | | | | | | | |
| O(7) | 1.436(8) | | | | | | |
| O(8) | 1.441(9) | 112.8(6) | 2.396(12) | | | | |
| O(9) | 1.452(10) | 113.0(6) | 2.409(13) | 112.0(6) | 2.398(14) | | |
| $O(10)_D$ | 1.580(8) | 107.1(5) | 2.427(12) | 104.3(5) | 2.387(12) | 107.0(5) | 2.439(12) |
| $\sum S = 6.02$ | $\langle 1.477 \rangle$ | O(7) | O(7) | O(8) | O(8) | O(9) | O(9) |

* Excluded from calculation of average Cs(2)–O distance.

hydrogen-bonded atoms increased by approximately 0.01 Å upon introduction of the hydrogen atoms into the structural model.

At this stage, an attempt was made to refine the structure in space group *Cc*. The absence of inversion symmetry in the structure would imply that the H(1), H(3), and H(4) atoms

**TABLE 5**
**Interatomic Distances (Å) and Angles (deg) between Atoms Involved in Hydrogen Bonds in $Cs_5(HSO_4)_3(H_2PO_4)_2$[a]**

| | O neighbors | $\sum S(O_D)$ | $\sum S(O_A)$ | $d(O \cdots O)$ (Å) | $d(O_D–H)$ (Å) | $d(O_A \cdots H)$ (Å) | $\angle O_DHO_A$ (deg) | $\angle XO_DH$ (deg) | $\sum S(H)$ |
|---|---|---|---|---|---|---|---|---|---|
| H(1) | $O(3)_{A/D}$–$O(3')_{A/D}$ | 1.54/1.93 | [1.54/1.93] | 2.589(18) | 1.295 | [1.295] | 180 | 118.6 | 0.78 |
| H(2) | $O(10)_D$–$O(1)_A$ | 1.30/2.07 | 1.65/1.84 | 2.578(12) | 1.021 | 1.590 | 161.3 | 108.5 | 0.96 |
| H(3) | $O(2)_{A/D}$–$O(2')_{A/D}$ | 1.54/1.88 | [1.54/1.88] | 2.517(15) | 1.259 | [1.259] | 180 | 118.0 | 0.85 |
| H(4) | $O(4)_{A/D}$–$O(4')_{A/D}$ | 1.61/2.05 | [1.61/2.05] | 2.483(17) | 1.241 | [1.241] | 180 | 115.9 | 0.89 |
| H(5) | $O(6)_D$–$O(5)_A$ | 1.45/1.95 | 1.54/1.94 | 2.482(13) | 1.119 | 1.285 | 175.1 | 122.4 | 0.89 |

[a] H(1), H(3) and H(5) constrained to reside on center of symmetry. Sum of the bond valences at the oxygen atom sites, both excluding and including protons, and at the proton sites also provided. Bond strengths for O–H bonds calculated according to $S(O–H) = \exp[(0.914–d_{O–H})/0.404]$ (14).

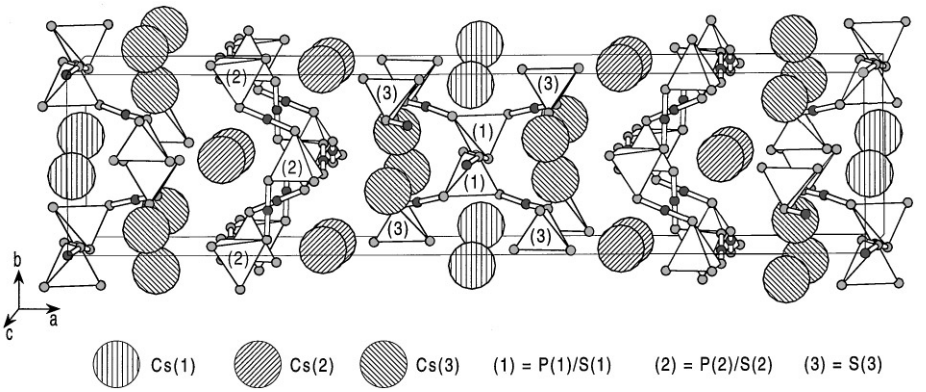


**FIG. 1.** Structure of $Cs_5(HSO_4)_3(H_2PO_4)_2$ viewed along *c*.

do not reside in symmetric potential wells, and would allow for the possibility of room-temperature ferroelectric behavior in $Cs_5(HSO_4)_3(H_2PO_4)_2$. Refinements without the incorporation of structural constraints in this low symmetry space group were, not surprisingly, unstable because of the high correlations between the respective coordinates and thermal parameters of pseudosymmetry-related atoms. On the other hand, refinements in which sufficient constraints were applied so as to maintain stability yielded inconclusive results. Therefore, while one cannot rule out the possibility that the compound crystallizes in space group *Cc*, space group *C*2/*c* adequately describes the X-ray structure and is assumed from here on.

## DISCUSSION OF STRUCTURE

### *General Features*

The general features of the structure of $Cs_5(HSO_4)_3(H_2PO_4)_2$ are shown in Fig. 1, in which Cs atoms and protons are depicted as spheres, $XO_4$ groups are depicted as tetrahedra, and oxygen atoms at the corners of the $XO_4$ tetrahedra are shown as spheres. Bonds shown are those between hydrogen and oxygen atoms. It is apparent from this figure that the structure is composed of alternating layers of $(CsHXO_4)_3$ and $(CsH_2XO_4)_2$, that are parallel to (100). Furthermore, hydrogen bonds are formed only within the individual $(CsHXO_4)_3$ and $(CsH_2XO_4)_2$ layers and not between them. The arrangement of cations and $XO_4$ anion groups in the $(CsHXO_4)_3$ portion of the structure is almost identical to that found in $CsHSO_4$-II (16), the midtemperature phase of cesium hydrogen sulfate, Fig. 2, whereas the arrangement in the $(CsH_2XO_4)_2$ portion of the structure is almost identical to that found in $CsH_2PO_4$ (8) and in $CsHSO_4$-III (7), the room-temperature phase of cesium hydrogen sulfate, Fig. 3.

### *$CsHSO_4$-Like Region*

Within the $(CsHXO_4)_3$ layers, sulfate/phosphate groups are arranged in zigzag rows that extend along [001] and alternate in a checkerboard fashion with zigzag rows of Cs cations that also extend along [001]. Two crystallographically distinct $XO_4$ row types are present, as are two crystallographically distinct Cs row types. The first $XO_4$ row, formed by $X(1)O_4$ tetrahedra, is located at the centers and edges of the unit cell, Fig. 1. All four oxygen atoms of the $X(1)O_4$ anion groups participate in forming hydrogen

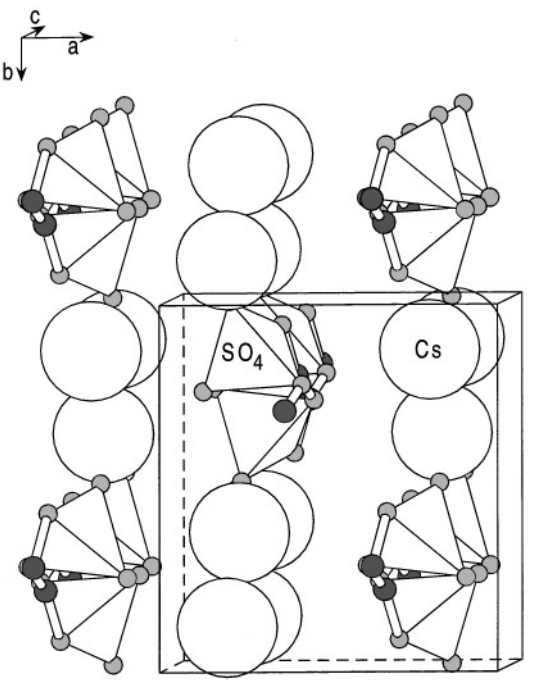


**FIG. 2.** Structure of $CsHSO_4$-II (14) viewed along *c*. Note the similarity between this and the $(CsHXO_4)_3$ region of $Cs_5(HSO_4)_3(H_2PO_4)_2$ (Fig. 1). Black spheres represent protons and grey spheres oxygen atoms.

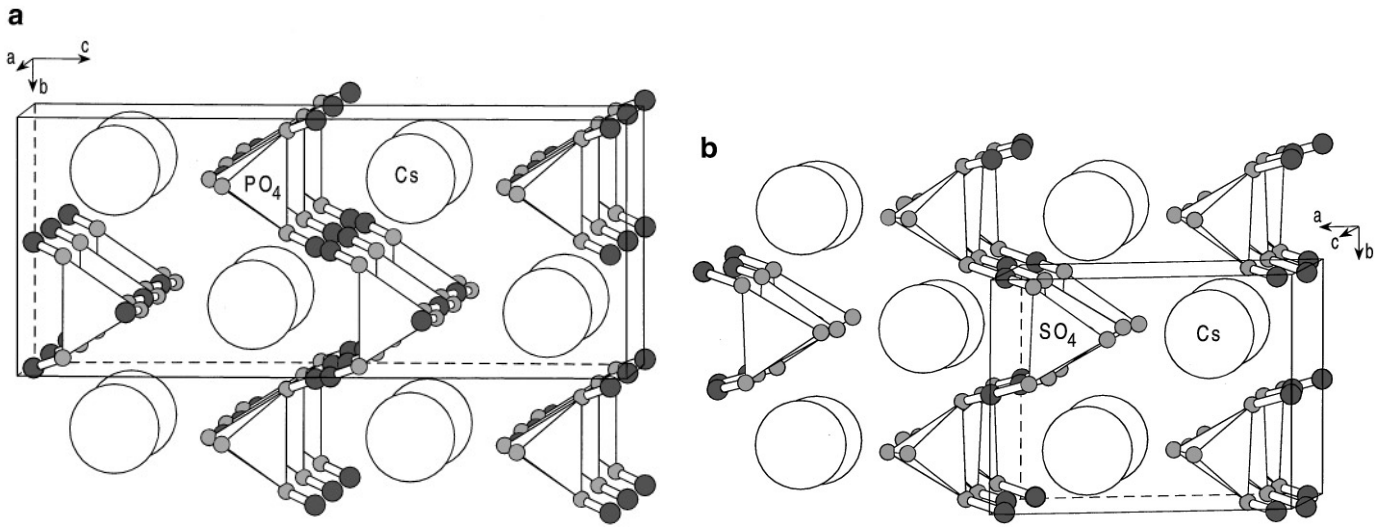


**FIG. 3.** Structures (a) of $CsH_2PO_4$ (8) and (b) of $CsHSO_4$-III (7), each shown along a direction that emphasizes the similarities between the compound and the $(CsH_2XO_4)_2$ region of $Cs_5(HSO_4)_3(H_2PO_4)_2$ (Fig. 1). Black spheres represent protons and grey spheres oxygen atoms.

bonds. Those bonds that link $X(1)O_4$ groups along the length of the chain, O(2)–H(3)–O(2′), are symmetric, whereas those linking $X(1)O_4$ to $S(3)O_4$ side groups, O(1)–H(2)–O(10), are asymmetric. In the second $XO_4$ row, that formed by $S(3)O_4$ tetrahedra, there are no hydrogen bonds along the direction of the row extension. The single hydrogen bond that is formed (at the O(10) donor oxygen atom) serves to link the $S(3)O_4$ anions to the $X(1)O_4$ chain.

The overall hydrogen-bond linkage between $XO_4$ groups in the $CsHSO_4$-like region of the structure is illustrated in Fig. 4a, a projection along *b* of a portion of the structure. From this figure it is apparent that the $XO_4$ groups are hydrogen-bonded to form a branched, linear chain, with branches that alternately extend above and below the main backbone of the chain. A thermal ellipsoid projection of the atoms that form this chain is shown in Fig. 4b. The figure demonstrates that all oxygen thermal vibrations are greatest along directions perpendicular to the direction of the *X*–O bonds, and that the oxygen atom at the end of the branch, O(7), undergoes the greatest thermal motion, as would be expected for such a structure. Moreover, the thermal motions of the *X* atoms are relatively isotropic.

Alternating zigzag rows of $XO_4$ groups and of Cs cations, as identified in the structure of $Cs_5(HSO_4)_3(H_2PO_4)_2$, have also been observed in $\alpha$-$Cs_3(HSO_4)_2(H_2PO_4)$ (17) and in $\beta$-$Cs_3(HSO_4)_2(H_{2-x}(P_{1-x}S_x)O_4)$ (18). The very small differences between the structural arrangements in these three structures and in $CsHSO_4$-II (16) demonstrate that this "alternating zigzag chain" motif is thermodynamically quite favorable in acid sulfates and phosphates containing large counter cations, and does not require any specific distribution of hydrogen bonds in order to stabilize it.

### *$CsH_2PO_4$-Like Region*

Within the $(CsH_2XO_4)_2$ layers of $Cs_5(HSO_4)_3(H_2PO_4)_2$ the $XO_4$ groups form rows that, again, extend along [001]. In this case, however, the rows are rather straight and contain only one crystallographically distinct $XO_4$ anion, $X(2)O_4$. Moreover, these $XO_4$ groups are hydrogen-bonded to one another by asymmetric hydrogen bonds to form $HXO_4$ chains, which are, in turn, linked by two crystallographically distinct types of symmetric hydrogen bonds to form $H_2XO_4$ layers that lie parallel to (100). Thus, all oxygen atoms of the $X(2)O_4$ tetrahedra participate in the formation of hydrogen bonds.

The structure of the $CsH_2XO_4$ layer in $Cs_5(HSO_4)_3(H_2PO_4)_2$ is illustrated in Fig. 5a in projection along *a*. A thermal ellipsoid representation of the atoms that comprise this layer is depicted in Fig. 5b. A comparison of Fig. 4b and 5b (and examination of Tables 2 and 3) reveals that, overall, the thermal displacements are greater in the phosphate-like region of the structure than in the sulfate-like region. This may be the result of the H(1) and H(4) protons being disordered such that each resides at two positions slightly displaced from the inversion centers (at which they were constrained to reside), or the result of a reduction in the local symmetry from $C2/c$ to $Cc$ if the protons are displaced from the apparent inversion centers in an asymmetric fashion. Nevertheless, the phosphorous/sulfur (and cesium) atoms exhibit essentially isotropic vibrations and, again, the greatest thermal displacements of oxygen atoms are perpendicular to the *X*–O bond direction.

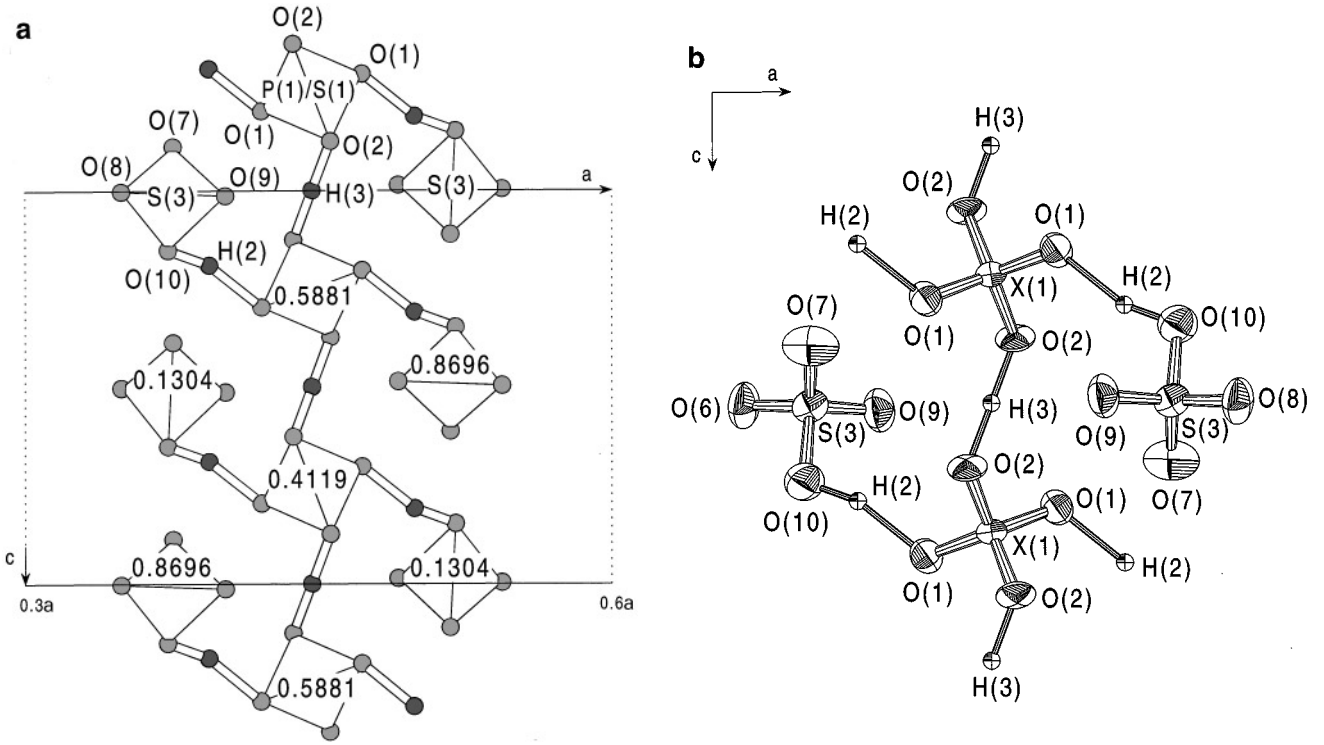


**FIG. 4.** (a) Projection of a portion of the structure of $Cs_5(HSO_4)_3(H_2PO_4)_2$ along *b* showing the branched hydrogen-bonded chain formed by $X(1)O_4$ and $S(3)O_4$ groups. Elevation of central phosphorous and sulfur atoms as indicated. (b) Thermal ellipsoid representation (with an electron probability of 50%) of a similar portion of the structure.

*Comparisons with Related Structures*

In Fig. 6 the relevant features (distances and angles) of the $XO_4$ rows observed in cesium acid sulfate/phosphates are illustrated. A quantitative comparison of the structures of $Cs_5(HSO_4)_3(H_2PO_4)_2$, $\beta$-$Cs_3(HSO_4)_2(H_{2-x}(P_{1-x}S_x)O_4)$, $\alpha$-$Cs_3(HSO_4)_2(H_2PO_4)$, $CsHSO_4$-II, $CsHSO_4$-III, and $CsH_2PO_4$ in terms of these features is provided in Table 6. From these data, it is evident that the zigzag $XO_4$ rows formed in the $CsHSO_4$-like region of $Cs_5(HSO_4)_3(H_2PO_4)_2$ are rather strained compared to those formed in the related compounds. The average distance between *X* atoms along the two types of rows in the former is 4.886 Å as compared to ~4.4 Å for $CsHSO_4$-III, $\beta$-$Cs_3(HSO_4)_2(H_{2-x}(P_{1-x}S_x)O_4)$, and $\alpha$-$Cs_3(HSO_4)_2(H_2PO_4)$. The large $X$–$X$ distance in $Cs_5(HSO_4)_3(H_2PO_4)_2$ cannot be attributed to the incorporation of P onto these sites as both $\beta$-$Cs_3(HSO_4)_2(H_{2-x}(S_xP_{1-x})O_4)$ and $\alpha$-$Cs_3(HSO_4)_2(H_2PO_4)$ also contain phosphate groups in their respective zigzag rows. This increase in the $X$–$X$ distance is accompanied by a straightening out of the rows, i.e., there is an increase in the $X$–$X$–$X$ angle, a reduction in the *b* lattice constant, and an increase in the repeat distance along the direction of the row. Such distortions are necessary to accommodate the $CsH_2PO_4$-like region of $Cs_5(HSO_4)_3(H_2PO_4)_2$. In the end-member phosphate, in which the phosphate chains are expected to be unstrained, the $PO_4$ row repeat distance is 4.873 Å, whereas for $Cs_5(HSO_4)_3(H_2PO_4)_2$ it is 4.579 Å. The analogous distance in $CsHSO_4$-III is significantly longer, 5.492 Å, presumably because there are no hydrogen bonds linking the $SO_4$ along the chain direction. The reduction in the $XO_4$ repeat distance in $Cs_5(HSO_4)_3(H_2PO_4)_2$ as compared to $CsH_2PO_4$ is accompanied by an increase in the *b* lattice constant, from 6.389 Å (in $CsH_2PO_4$) to 7.661 Å (in $Cs_5(HSO_4)_3(H_2PO_4)_2$), a value that matches that of the $CsHSO_4$-like portion of the structure. Again, it is unlikely that this increase is due to the incorporation of sulfur into the $CsH_2PO_4$-like portion of the structure.

The strains in the structure of $Cs_5(HSO_4)_3(H_2PO_4)_2$ relative to the end-member sulfate and phosphate can then be roughly summarized as follows. In the $CsHSO_4$-like portion of the structure, there is ~10% elongation along the $XO_4$ and Cs row direction and ~5% compression in the *b* lattice constant; in the $CsH_2PO_4$-like region of the structure, there is ~7% compression along the $XO_4$ and Cs row direction and ~15% elongation in the *b* lattice constant. Overall, the volume per $CsHXO_4$ group in $Cs_5(HSO_4)_3(H_2PO_4)_2$ is significantly larger than in the related solid acid

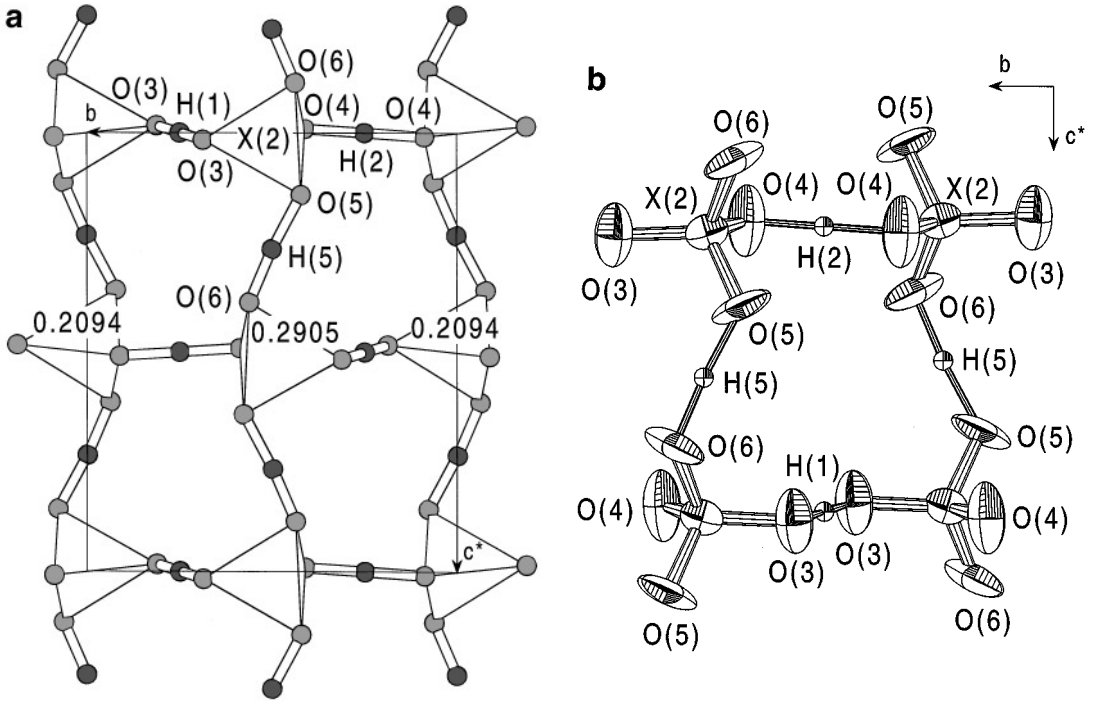


**FIG. 5.** (a) Projection of the structure of $Cs_5(HSO_4)_3(H_2PO_4)_2$ along $a$, from $x = 0.15$ to 0.35, showing the hydrogen-bonded layer formed by $X(2)O_4$ groups. Elevation of central phosphorous/sulfur atoms as indicated. (b) Thermal ellipsoid representation (with an electron probability of 50%) of a similar portion of the structure.

sulfate/phosphates, with the $CsH_2PO_4$-like portion of the structure under particularly large tensile stresses. The expansion of the structure in this region may be, in part, responsible for the much larger thermal parameters apparent for the atoms represented in Fig. 5b than for those in Fig. 4b. The structural stresses may also explain why a hydrogen bond is formed between O(1) and O(10) rather than between O(9) and O(8) in the $CsHSO_4$-like region of the structure. Such a rearrangement of the hydrogen bonds (from O(1)–O(10) to O(9)–O(8)) would lead to greater uniformity in the distribution of hydrogen bonds in the structure, as well as render this region much more similar to $CsHSO_4$-II. However, formation of an hydrogen bond between O(9) and O(8) is precluded by the great distance between these two oxygen atoms, which results from the large (relative to $CsHSO_4$-II) distance between $SO_4$ groups along the zigzag rows.

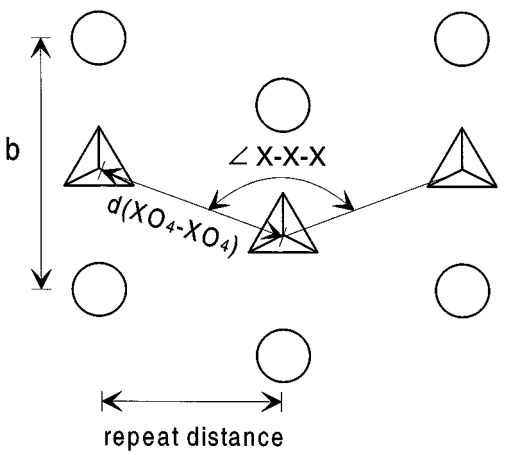


**FIG. 6.** Schematic illustration of the zigzag rows of $XO_4$ anions and Cs cations showing relevant distances and angles.

In comparison to other sulfate–phosphate compounds, the presence of a distinct sulfur site in $Cs_5(HSO_4)_3(H_2PO_4)_2$ is a somewhat surprising structural feature. The compounds $CaAl_3(PO_4)(SO_4)(OH)_6$ (19), $SrAl_3(PO_4)(SO_4)(OH)_6$ (20), $Zr_2(PO_4)_2(SO_4)$ (21), $Pb_4(PO_4)_2(SO_4)$ (22), $K_2(HSO_4)_2(H_2PO_4)$ (23), and $(NH_4)_2(HSO_4)(H_2PO_4)$ (24) are all reported to have P and S on the same site, whereas only and $\alpha$-$Cs_3(HSO_4)_2(H_2PO_4)$, $\beta$-$Cs_3(HSO_4)_2(H_{2-x}(S_xP_{1-x})O_4)$, and $PbFe_3(SO_4)(PO_4)(OH)_6$ (25) are reported to contain an ordered or semiordered (in the case of $\beta$-$Cs_3(HSO_4)_2(H_{2-x}(S_xP_{1-x})O_4)$) arrangement of tetrahedral groups. The apparent absence of P/S ordering in so many sulfate–phosphate compounds may be an experimental artifact reflecting the difficulty of distinguishing between $P^{6+}$ and $S^{5+}$ with X-ray methods alone, rather than truly indicating disorder. The fact that in many of these

**TABLE 6**
**Comparison of Selected Structural Features of $Cs_5(HSO_4)_3(H_2PO_4)_2$, α-$Cs_3(HSO_4)_2(H_2PO_4)$ (15), β-$Cs_3(HSO_4)_2(H_{2-x}(P_{1-x}S_x)O_4)$ (16), $CsDSO_4$-II (14), $CsHSO_4$-III (7), and $CsH_2PO_4$ (8); See Fig. 6 for a Definition of Geometric Parameters**

| Property | $CsDSO_4$-II | α-$Cs_3$.. | β-$Cs_3$.. | $Cs_5$.. | $CsHSO_4$-III | $CsH_2PO_4$ | $Cs_5$.. |
|---|---|---|---|---|---|---|---|
| Distribution of P and S sites | All S | 2 S, 1 P | 2 S, 1 (P,S) | 1 S, 2 (P,S) | All S | All P | |
| H : $XO_4$ | 1 : 1 | 4 : 3 (1.33) | ~7 : 6 (1.17) | 7 : 5 (1.4) | 1 : 1 | 2 : 1 | |
| H bonds/$XO_4$ | 2/$SO_4$ | 4/$PO_4$<br>2/$SO_4$ | 4/(P,S)$O_4$<br>~1.5/$SO_4$ | 4/(P,S)$O_4$<br>1/S(2)$O_4$ | 2/$SO_4$ | 4/$PO_4$ | |
| Dimensionally of H-bond network | 1 | 3 | 3 (weak) | 2 & 1-branched | 1 | 2 | |
| Nature of H bonds | Ordered | Ordered and disordered | Ordered and disordered, vacancies | Ordered and disordered | Ordered | Ordered and disordered | |
| Volume/$CsH_xXO_4$, Å$^3$ | 114.3 | 115.9 | 115.6 | 119.4 | 114.2 | 116.8 | |
| *b*-lattice parameter, Å | 8.13916 | 7.8798 | 7.854 | 7.661 | 5.809 | 6.3689 | |
| Chain/row property | Zigzag chains/rows | | | | Straight chains/rows | | |
| Average $d(XO_4$–$XO_4)$ along chain, Å | 4.340 | 4.383 | 4.424 | 4.886 | 5.494 | 4.873 | 4.580 |
| $\angle X$–$X$–$X$, deg | 127.5 | 122.9 | 123.6 | 140.0 | 176.6 | 180 | 177.7 |
| Repeat distance, Å | 3.861 | 3.844 | 3.890 | 4.579 | 5.492 | 4.873 | 4.579 |

compounds more than one (P, S) site exists and the P : S ratio could be achieved by an ordered distribution on these sites, further suggests experimental limitations rather than true disorder.

A second interesting feature of the compounds in the $CsHSO_4$–$CsH_2PO_4$ system is their existence over exceeding small composition ranges: within experimental error, α-$Cs_3(HSO_4)_2(H_2PO_4)$ and $Cs_5(HSO_4)_3(H_2PO_4)_2$ crystallize as line compounds, and even β-$Cs_3(HSO_4)_2(H_{2-x}(S_xP_{1-x})O_4)$, with a site confirmed by neutron diffraction studies (26) to be occupied by both P and S, exists over a narrow P : S range. While solid solubility regions in sulfate–phosphate compounds have not generally been studied, it is noteworthy that in the $Li_2SO_4$–$Li_3PO_4$ system, for which the phase diagram has been published (27), at temperatures less than 561°C, P is essentially insoluble in $Li_2SO_4$-II (within a detection limit of approximately 1 mol%). Above 561°C the sulfate transforms to phase I and the solubility increases, becoming significant only at temperatures above ~700°C. Moreover, $Li_2SO_4$ is insoluble in any of the phases of $Li_3PO_4$ over the temperature range examined, 400–950°C. In a more closely related system, D'Yvoire and co-workers investigated phase formation in $x$KHSO$_4$–$(1-x)$K$H_2PO_4$ and have reported the existence of two compounds in addition to the end-members (28). The first is a line compound, $KHSO_4 \cdot KH_2PO_4$ (presumably the same phase as that reported by Averbuch-Pouchot and Durif (23)), and the second a compound of variable composition that exists over the range from $KHSO_4 \cdot 3KH_2PO_4$ to $KHSO_4 \cdot 7KH_2PO_4$. Unfortunately, little is known of this latter phase. O'Keeffe and Perrino carried out a systematic study of the conductivity of $KHSO_4$-doped $KH_2PO_4$ and observed that the maximum solubility of sulfur in the phosphate is only ~0.8 mol% (29). Thus, it appears that both line compounds and compounds of variable composition can be obtained in these systems. Identification of the phases in which the proton content can be tuned so as to obtain desirable transport properties will be critical to designing materials with high proton conductivity.

### *Hydrogen-Bond Geometry*

It is well-known that $X$–$O_D$ distances are, in general, longer than $X$–O and $X$–$O_A$ distances (where $O_D$ and $O_A$ are donor and acceptor oxygen atoms, respectively, in the $O_D$–H ⋯ $O_A$ bond). It is also rather well-established that, as the distance between two hydrogen bonded oxygen atoms decreases, the $X$–$O_D$ distance decreases, such that the difference between the $X$–$O_D$ and $X$–$O_A$ distances decreases. That is to say, as the hydrogen bond becomes stronger and the two H-bonded oxygen atoms approach one another, the distinction between donor and acceptor decreases. Decreases in the $O_A$ ⋯ $O_D$ bond distance are also accompanied by a decrease in the difference between the H–$O_D$ and H ⋯ $O_A$ distances, and there is a tendency for very strong hydrogen bonds to be symmetric (30).

In our investigation of the structure of α-$Cs_3(HSO_4)_2(H_2PO_4)$, use of literature tabulated correlations between P–$O_D$, P–O, and $O_A$ ⋯ $O_D$ distances and between S–$O_D$ and $O_A$ ⋯ $O_D$ proved a powerful tool for identifying donor, acceptor, and non-hydrogen-bonded oxygen atoms (17). It was noted at that time, however, that while Ichikawa (31), in

his examination of bond distances in phosphates, differentiated between $PO_4$ groups with differing numbers of donor oxygen atoms, Catti *et al.* (32) made no such distinction between different types of $SO_4$ groups in their study of S–OH distances. Moreover, Ichikawa demonstrated that P–O bond lengths (that is, the bonds between phosphorus and non-hydrogen bonded oxygen atoms) in $PO_3(OH)$, for example, are also correlated to $O_D \cdots O_A$ distances, as a result of the influence of the latter on $P–O_D$ bond lengths and the tendency for the phosphate ion to maintain a constant average value of all four phosphorous–oxygen distances, Fig. 7. It is reasonable to expect that such a correlation should also exist in sulfates, but no systematic study has been carried out. For these reasons, and because several accurate structure determinations of new, inorganic solid-acid sulfates have recently appeared in the literature, we have re-examined the correlation between sulfur–oxygen distances and oxygen–oxygen distances.

Scatter diagrams of S–O, $S–O_A$, and $S–O_D$ vs $O_A \cdots O_D$ for $SO_3(OH)$ tetrahedral groups are presented in Fig. 8a–c, respectively.[3] Only data for structures in which $R(F)$ was less than 0.05, and in which $O \cdots O < 2.8$ Å are included. In Fig. 8a the S–O distance is the average of the distances between sulfur and the three nondonor oxygen atoms. Acceptor oxygen atoms have been included in determining this average. In Fig. 8b the possible correlation of $S–O_A$ distances, where the $O_A$ participate in some other hydrogen bond than the $O_A \cdots O_D$ bond of interest, is examined separately. In this case, one oxygen atom is a donor and at least one is an acceptor; the number of additional acceptor oxygen atoms is indicated. Figure 8a and c can be compared to Fig. 1 of Ichikawa (31), in which similar results of $PO_3(OH)$ groups are presented. In Fig. 8d the linear regression lines obtained in this study are directly compared with those determined by Ichikawa (31) for both $PO_3(OH)$ and $PO_2(OH)_2$ groups and by Catti *et al.* (32) for S–OH vs $O \cdots O$.

Fig. 8a reveals a very slight dependence of S–O on $O \cdots O$, Fig. 8b demonstrates that $S–O_A$ is virtually independent of the $O \cdots O$ distance, but is somewhat sensitive to the number of acceptors, whereas Fig. 8c shows that $S–O_D$ increases demonstrably with increasing $O \cdots O$, in general agreement with the results of Catti *et al.* (32), and in analogy to the behavior of the phosphate ion. Kemnitz *et al.* (33), who recently examined S–O and S–OH distances as a function of the role played by the oxygen atoms in the coordination polyhedron about the counter cation, have concluded that $S–O_A$ distances are typically 0.015 Å longer than S–O distances and that the range of values for each type of bond overlap significantly. Such a conclusion can also be drawn from the data in Fig. 8a and b. Most significantly, the linear regression curve determined in this study for $S–O_D$ as a function of $O \cdots O$ has a shallower slope than that obtained by Catti *et al.* and parallels closely the result of Ichikawa for $HPO_4$. Similarly, the S–O regression line parallels that of P–O, while the absolute difference between S–O and P–O is much greater than that between $S–O_D$ and $P–O_D$.

[3] A list of bond lengths and the structural papers from which they were obtained has been deposited. See footnote 2 for ordering information.

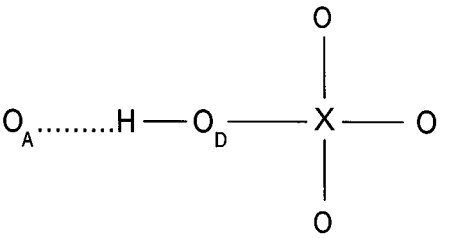


**FIG. 7.** Schematic illustration of the $O_A \cdots H–O_D–XO_3$ geometry. As the strength of the hydrogen bond increases, the $O_A \cdots O_D$ distance decreases, inducing an increase in the $O_D$–H distance, a decrease in the $X–O_D$ distance, and, in turn, an increase in the $X$–O distances.

The scatter diagrams of Fig. 8a–c do not include data from $Cs_5(HSO_4)_3(H_2PO_4)_2$. These data points are compared to the linear regression curves for $SO_3(OH)$ (present work) and $PO_2(OH)_2$ (Ichikawa) in Fig. 9. The hydrogen bond of relevance to the $X(1)O_4$ group is the O(2)–O(2′) bond about H(3). Points a and b on Fig. 9 represent $X(1)$–O(1) vs O(2)–O(2′) and $X(1)$–O(2) vs O(2)–O(2′) distances, respectively. For the $X(2)O_4$ group, there are three relevant hydrogen bonds, about H(1), H(4), and H(5), and the average of the three corresponding O–O distances is 2.518(15) Å. Points c–f represent the four $X(2)$–O distances, $X(2)$–O(6), $X(2)$–O(5), $X(2)$–O(4), and $X(2)$–O(3), respectively vs this average hydrogen bond distance. The $S(3)O_4$ group is involved in only one hydrogen bond, H(2), for which O(10) serves as a donor. Accordingly, points g–j represent the S(3)–O distances, S(3)–O(10), S(3)–O(9), S(3)–O(8), and S(3)–O(7), respectively, vs the O(10)–O(1) distance. For simplicity, acceptor oxygen atoms are treated essentially as non-hydrogen bonded atoms, an approach justified by the similarity of S–O and $S–O_A$ distances noted in Fig. 8a and b. The nature of the $X(2)O_4$ group, with two mixed donor/acceptor atoms and one donor oxygen atom, suggests that a comparison of its bond distances to regression curves determined for $SO_2(OH)_2$ (in addition to those for $PO_2(OH)_2$) would be desirable. However, the limited number of compounds containing this unit prevented the generation of meaningful scatter diagrams. Nevertheless, Kemnitz *et al.* (33) have shown that the average S–OH distance in $SO_2(OH)_2$ is shorter by 0.031 Å than that in $SO_3(OH)$, and, similarly, S–O is shorter by 0.024 Å.

The data presented in Fig. 9 support the assumptions made regarding the location of protons and the distribution of sulfur and phosphorus in the $X$ atom sites. The identification of the second 8*f* atom site (Table 2) as sulfur, S(3), is

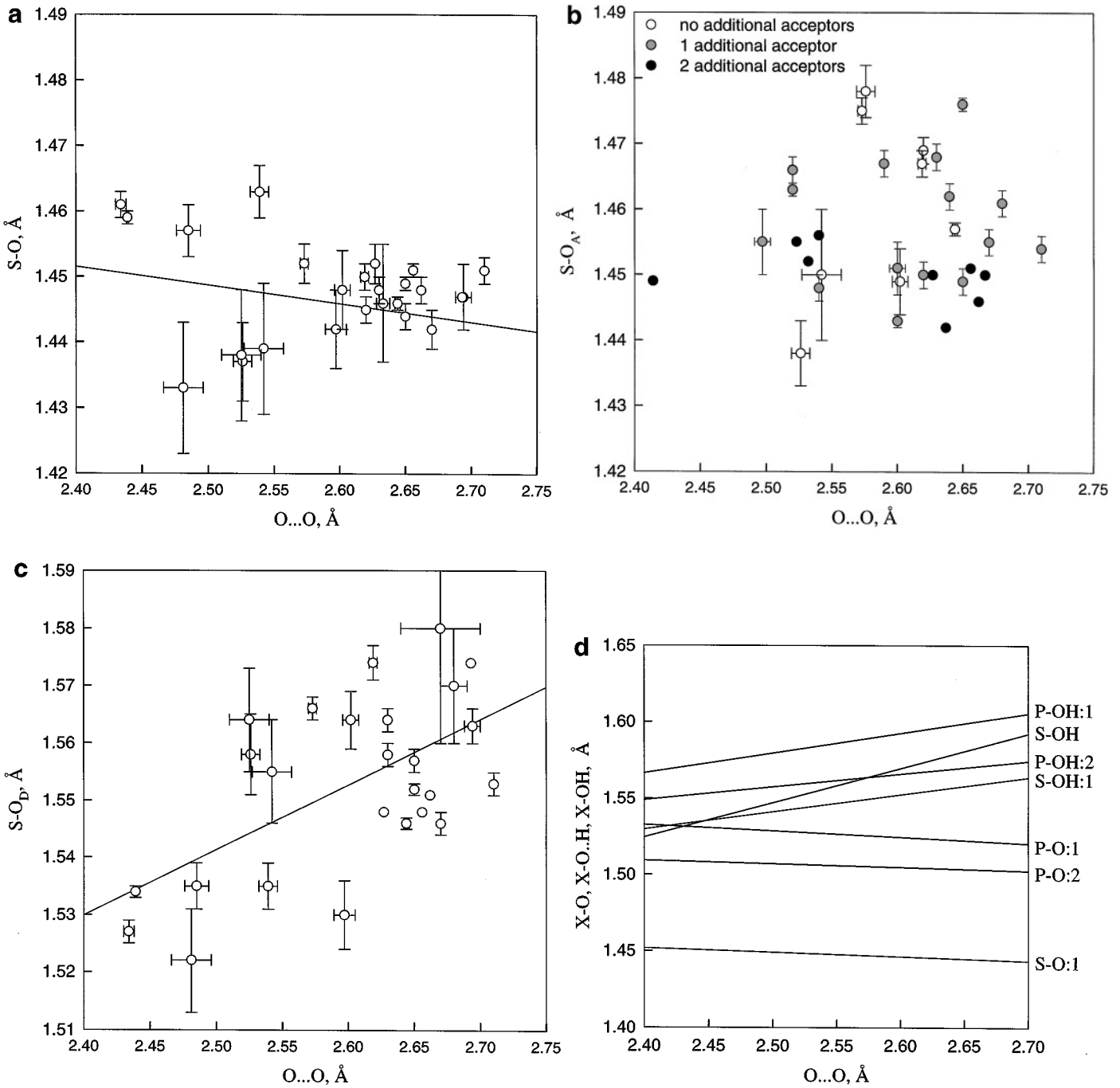


**FIG. 8.** Scatter diagrams of (a) S–O vs O ⋯ O, (b) S–O ⋯ H vs O ⋯ O, and (c) S–OH vs O ⋯ O in single donor $SO_4$ (i.e. $SO_3(OH)$) groups and (d) a comparison of the linear regression curves obtained in the present work with earlier results. Error bars reflect the reported esd for the bond length in question, with the following exception: for S–O vs O ⋯ O data points, the average of all nondonor oxygen to sulfur distances has been utilized, and the error bars reflect the maximum esd in any one of those distances. For the S–O ⋯ H vs O ⋯ O scatter diagram, data were taken from sulfate groups in which at least one of the three nondonor oxygen atoms in an acceptor. The number of additional acceptors is indicated. Linear regression curves are (a) S–O = 1.519(O ⋯ O) − 0.028; and (c) S–OH = 1.242(O ⋯ O) + 0.120. In (d) the number after *X*–OH indicates the number of donor oxygen atoms in the anion group. Sources: S–OH : 1, S–O : 1, this work; P–OH : 1, P–O : 1, P–OH : 2, P–O : 2, Ichikawa (31); S–OH, Catti *et al.* (32).

confirmed by the fact that the *X*–O bond distances (for oxygen atoms that do not participate in hydrogen bonding), points g–i, correspond to those expected for sulfur, and are significantly shorter than would be expected for phosphorus. The rather long S(3)–O(10) distance indicates that the O(1)–O(10) bond is slightly weaker and the O(10)–H(2)

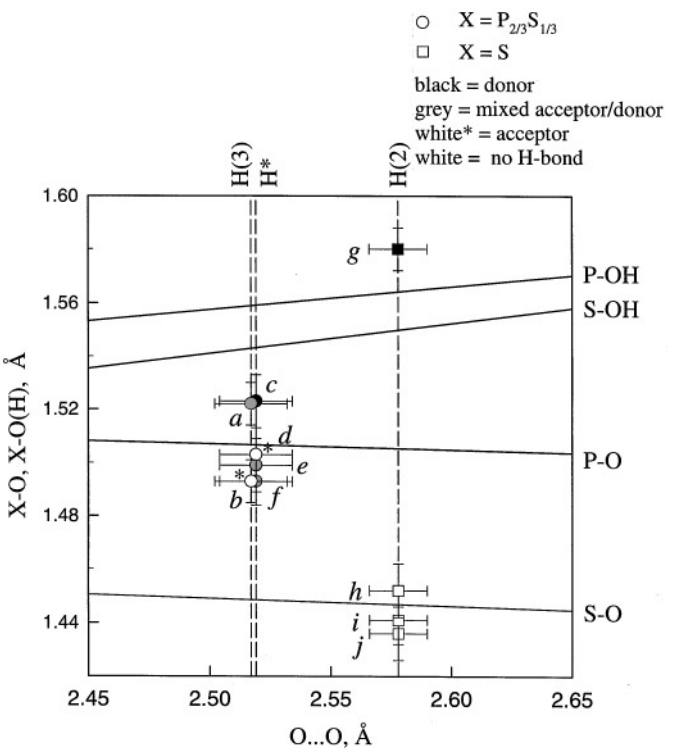


**FIG. 9.** The $X$–O vs O ⋯ O data points of $Cs_5(HSO_4)_3(H_2PO_4)_2$ as compared to the linear regression curves for $SO_3(OH)$ and $PO_2(OH)_2$. In the case of $X(2)O_4$, in which three oxygen atoms serve as either donor atoms or mixed acceptor/donor atoms in a hydrogen bond, the O ⋯ O distance utilized is the average, ⟨O ⋯ O⟩, of O(3) ⋯ O(3), O(4) ⋯ O(4), and O(5) ⋯ O(6) and is represented by H* in the figure. Data points refer to the following bond distance pairs: (a)= $X(1)$–$O(2)_{A/D}$ vs O(2) ⋯ O(2); (b) $X(1)$–$O(1)_A$ vs O(2) ⋯ O(2); (c) $X(2)$–$O(6)_D$ vs ⟨O ⋯ O⟩; (d) $X(2)$–$O(5)_A$ vs ⟨O ⋯ O⟩; (e) $X(2)$–O(4) vs ⟨O ⋯ O⟩; (f) $X(2)$–O(3) vs ⟨O ⋯ O⟩; (g) S(3)–$O(10)_D$ vs O(1)–O(10); (h) S(3)–O(9) vs O(1)–O(10); (i) S(3)–O(8) vs O(1)–O(10); (j) S(3)–O(7) vs O(1)–O(10).

bond slightly stronger than expected on the basis of the O(1)–O(10) distance alone. This is reflected in the sum of the bond valence at O(10): excluding H(2) it has the rather small value 1.30, but increases to a reasonable value of 2.07 when the contribution of the proton is included, Table 5.

In the case of the $X(2)O_4$ group, points c–f, the difference between $X$–$O_D$ and $X$–$O_A$ bond lengths is not as large as expected on the basis of the O ⋯ O distance. This, in turn, implies that the $O_D$–H bond, in this case O(6)–H(5), is not as strong as suggested by the O ⋯ O distance. Moreover, the $X$–$O_A$ length, point d, is essentially equal to that of the $X$–$O_{A/D}$ lengths, points e and f. These results suggest that the four oxygen atoms participate rather equally in the formation of hydrogen bonds, despite the differences in their formal definitions as donor, mixed acceptor/donor and acceptor atoms. The sum of the bond valences at these oxygen atoms, excluding proton contributions, are 1.45 for O(6) [point c], 1.54 for O(5), [point d], 1.61 for O(4) [point e], and 1.54 for O(3) [point f], values that are quite similar to one another and consistent with the picture of hydrogen bonds of relatively equal strength. In the $X(3)O_4$ group, the differences between the $X$–$O_{A/D}$ and $X$–$O_A$, points a and b, are slightly larger than in the case of $X(2)O_4$. Moreover, this difference is approximately what would be expected on the basis of the O(2)–O(2′) distance about H(3).

Returning to the question of whether the proton that reside in the symmetric bonds in $Cs_5(HSO_4)_3(H_2PO_4)_2$ are ordered, i.e. reside precisely at the center of symmetry, in a single-minimum potential well, or are disordered, i.e., reside at either side of the center of symmetry, in a double-minimum potential well, the long O ⋯ O distances about H(1), H(3), and H(4), 2.589(18), 2.517(15), and 2.483(17) Å, respectively, suggest that the first two and possibly all three should be disordered. In addition, the large thermal parameters of the mixed acceptor/donor atoms O(2) and O(3), bonded to H(1) and H(4), respectively, are also suggestive of local disorder, as stated earlier. Large atomic displacement parameters are expected for the double-minimum configuration because, at any given instant and for any given bond, each acceptor/donor atom should exist as either acceptor or donor, but not both. That is, bonds should have the form $X$–$O_D$–H ⋯ $O'_A$–$X'$ or $X$–$O_A$ ⋯ H–$O'_D$–$X'$, to yield a diffraction average of $X$–$O_{A/D}$–$H_{1/2}$ ⋯ $H'_{1/2}$–$O'_{A/D}$–$X'$. The averaging of the $X$–$O_A$ and $X$–$O_D$ distances would result in apparently large thermal parameters. Disorder at H(1) and H(4) is, however, inconsistent with the small $X$–O distances observed in the relevant $X$–$O_{A/D}$–H–$O'_{A/D}$–$X'$ bonds, Fig. 9. Short $X$–O distances normally accompany long O–H distances, which are more easily accommodated if the proton resides at the center of symmetry rather than displaced from it. Another useful measure for the likelihood of disorder is the sum of the bond strengths at the proton site under the assumption of complete order. In the case of H(1), this atom is severely underbonded when restricted to the center of symmetry. Because of the exponential nature of the bond strength, the $X$–$O_{A/D}$–$H_{1/2}$ ⋯ $H'_{1/2}$–$O'_{A/D}$–$X$ configuration yields a higher bond sum for both protons and oxygen atoms than the $X$–$O_{A/D}$–H–$O'_{A/D}$–$X'$ configuration. Thus, bond strength considerations indicate the H(1) proton should be disordered.

In summary, the large O ⋯ O distance, the large thermal parameters on O(3) and the severe underbonding at H(1) indicate that this proton should reside in a double-minimum rather than a single-minimum potential well. These factors outweigh the indication of a single-minimum potential well as determined from the short $X(2)$–O(3) distance. At H(3), the large O ⋯ O distance, the large $X(1)$–O(2) distance, and the underbonding at H(3) suggest a double-minimum potential well; however, the reasonable thermal displacement parameters determined for O(2) are suggestive

of a single-minimum potential well. The bond about H(4) is just at the lower limit of observed double-minimum symmetric potential wells, and the small $X(2)$–O(4) distance and the sum of the bond strengths at O(4) and H(4) suggest a single-minimum well. The large thermal parameters observed for O(4), however, favor a disordered model. Thus, while H(1) is almost undoubtedly disordered, further investigations are necessary to determine the structural arrangement about H(3) and H(4).

## PHASE TRANSITIONS, PROTON CONDUCTIVITY, AND FERROELECTRICITY

The manner in which $Cs_5(HSO_4)_3(H_2PO_4)_2$ accommodates the structural mismatches between the two almost discrete layers explains the rather surprising distribution of hydrogen bonds. The structure is unusual in that it contains an $SO_4$ group that participate in different numbers of hydrogen bonds: those at $S(3)O_4$ participate in only one, and those at $X(1)O_4$ and $X(2)O_4$ participate in four. For entropy reasons, one might expect all $SO_4$ anions to participate equally in the formation of hydrogen bonds. Indeed, in silicates, it is so well recognized that, for a given structure, the ratio of bridging to nonbridging oxygen atoms per $SiO_4$ group is generally a constant, that Liebau (34) has formulated his third "rule" for silicate anion topology on this basis. Applying this rationale to hydrogen bonded solids, we have proposed a model for describing superprotonic transition which simply states that the presence of oxygen atoms with different hydrogen bond environments is entropically unfavorable. Thus, at elevated temperatures all oxygen atoms participate, as uniformly as permitted, in the formation of hydrogen bonds. If the $H:XO_4$ ratio is not precisely equal to 2, the arrangement that provides for chemical equivalence between oxygen atoms necessarily involves structural disorder: either protons will reside the partially occupied sites or oxygen atoms will do the same, or both will do so. For example, $SO_4$ groups may take on multiple orientations, such that different oxygen atoms participate in H bonds in different orientations. Precisely this type of disorder is observed in the high-temperature, superprotonic structure of $CsHSO_4$ (phase I) (16). Moreover, it is precisely this type of disorder—sulfate groups undergoing rapid reorientation—that facilitates proton transport and results in high conductivity. In $Cs_5(HSO_4)_3(H_2PO_4)_2$ two types of sulfate groups exist, and the hydrogen bonding to these anions differs greatly. Thus, one might expect the driving force for a superprotonic transition, if such a transition exists, to be quite large, and to induce the phase change at a lower temperature than is observed in $CsHSO_4$.

In an alternative interpretation that does not address the driving force for superprotonic phase transitions, but does identify enabling structural features, Kreuer (35) has proposed that in order for $XO_4$ tetrahedra to undergo rapid reorientation, large counter cations, such as Rb, Cs, and Tl, are required. These species are believed to lower cation–anion and anion–anion bond strengths, promoting reorientational dynamics of the $XO_4$ anion, and also to lower proton–proton interactions, minimizing solvent effects. This conclusion is drawn, in part, from the observation that alkali acid sulfates of smaller alkali species do not undergo superprotonic phase transitions. In $Cs_5(HSO_4)_3(H_2PO_4)_2$ the large $XO_4$–$XO_4$ distance within the $(CsHXO_4)_3$ portion of the structure, as compared $CsDSO_4$-II, and the large volume per $CsH_xXO_4$ unit, as compared to any of the other structures, suggests that the overall bonding is rather weak. Thus, although the counter cation is the same as in $CsHSO_4$, it is reasonable to expect that a superprotonic phase transition should occur at a temperature lower than in the end-member sulfate.

Preliminary thermal analysis suggests that $Cs_5(HSO_4)_3(H_2PO_4)_2$ undergoes two phase transitions at approximately 116 and 137°C, with heats of transformation of 6.8 and 3.4 J/g, respectively (36). Although it is not yet known whether either is superprotonic transition, it has been confirmed that neither transition corresponds to decomposition as the DSC trace of a sample upon heating for a second time revealed the same two transitions, albeit at slightly lower temperatures. Experiments are presently underway to determine the nature of these transformations and their impact on conductivity. If the transition at 116°C does indeed correspond to the onset of superprotonic behavior, it would be an exciting confirmation that the structural prerequisites have been properly identified, and a demonstration that $T_C$ can be controlled by crystal-chemical design.

In addition to a superprotonic transition at elevated temperatures, many solid acid sulfates and phosphates exhibit ferroelectric transitions at low temperatures. Given the probable presence of disordered protons in $Cs_5(HSO_4)_3(H_2PO_4)_2$, it, too, is quite likely to undergo such a transition. Ichikawa *et al.* (37) have demonstrated that ferroelectric transition temperatures, within a given class of compounds, where a class is defined by the dimensionality of the disordered hydrogen-bond network, depend on O ⋯ O distances. The correlations these authors have put forth are difficult to utilize as predictive tools, however, because knowledge of the O ⋯ O distance at the transition temperature is required. Furthermore, in the present case, there may be as many as three disordered protons (forming one-dimensional chains along [010] and [001]), and it is unclear whether ordering at the H(1) and H(4) sites should occur at the same or at different temperatures. Nevertheless, low-temperature investigations of $Cs_5(HSO_4)_3(H_2PO_4)_2$ may provide important insight into ferroelectric phenomena.

## ACKNOWLEDGMENTS

This work was supported by the National Science Foundation through a National Young Investigator Award and by Battelle National Laboratories. The authors thank Scott Kuehner of the University of Washington for assistance with the microprobe analyses.

## REFERENCES

1. N. Bjerum, *Science* **115,** 385 (1952).
2. A. I. Baranov, L. A. Shuvalov, and N. M. Shchagina, *JETP Lett*. **36,** 459 (1982).
3. A. Pawlowski, Cz. Pawlaczyk, and B. Hilczer, *Solid State Ionics* **44,** 17 (1990).
4. B. V. Merinov, A. I. Baranov, L. A. Shuvalov, and N. M. Shchagina, *Sov. Phys. Crystallogr. (Engl. Transl.)* **36,** 321 (1991).
5. S. M. Haile, G. Lentz, K.-D. Kreuer, and J. Maier, *Solid State Ionics* **77,** 128 (1995).
6. S. M. Haile, P. M. Calkins, and D. Boysen, *Solid State Ionics* **97,** 154 (1997).
7. K. Itoh, T. Ozaki, and E. Nakamura, *Acta Crystallogr. Sect. B* **37,** 1908 (1981).
8. R. N. P. Choudhary and R. J. Nelmes, *Ferroelectrics* **21**(1–4), 443 (1978).
9. F. Schamber, N. Wodke, and J. McCarthy, "ZAF Matrix Correction Procedure for Bulk Samples: Operation and Program Description," 31 pp. Publication TN-2120, Tracor Northern, Middleton, WI 1981.
10. D. T. Cromer and J. T. Waber, "International Tables for X-ray Crystallography," Vol. IV, Table 2.2A, pp. 128–135. Birmingham, England, The Kynoch Press, 1974. [Present distributor: Kluwer Academic Publishers, Dordrecht]
11. G. M. Sheldrick, *in* "Crystallographic Computing 3" (G. M. Sheldrick, C. Kruger, and R. Goddard, Eds.), pp. 175–198. Oxford Univ. Press, New York, 1985.
12. G. M. Sheldrick, *in* "Crystallographic Computing 6" (H. D. Flack, L. Parkanyi, and K. Simon, Eds.), pp. 100–110. Oxford Univ. Press, New York, 1993.
13. I. D. Brown and D. Altermatt, *Acta Crystallogr. Sect. B* **41,** 244 (1985).
14. H. Alig, J. Lösel, and M. Trömel, *Z. Kristallogr.* **209,** 18 (1994).
15. M. Ichikawa, *Acta Crystallogr. B* **34,** 2074 (1978).
16. A. V. Belushkin, W. I. F. David, R. M. Ibberson, and L. A. Shuvalov, *Acta Crystallogr. B* **47,** 161 (1991).
17. S. M. Haile, K.-D. Kreuer, and J. Maier, *Acta Crystallogr. Sect. B* **51,** 680 (1995).
18. S. M. Haile, P. M. Calkins, and Dane Boysen, *J. Solid State Chem.* **139,** 373 (1998).
19. T. Kato, *Neues Jahrb. Mineral.-Monat*. (2) 54 (1977).
20. T. Kato and Y. Miura, *Miner. J. (Jpn.)* **8,** 418 (1977).
21. Y. Piffard, A. Verbaere, and M. Kinoshita, *J. Solid State Chem.* **71,** 121 (1987).
22. J. Barbier, *Eur. J. Solid State Inorg. Chem.* **31,** 563 (1994).
23. M. T. Averbuch-Pouchot and A. Durif, *Mater. Res. Bull.* **15,** 427 (1980).
24. M. T. Averbuch-Pouchot and A. Durif, *Mater. Res. Bull.* **16,** 407 (1981).
25. G. Giusepetti and C. Tadini, *Neues Jahrb. Mineral.-Monat*. (2) 71 (1987).
26. S. M. Haile and W. T. Klooster, in progress.
27. C. N. Wijayasekera and B. E. Mellander, *Solid State Ionics* **45,** 293 (1991).
28. F. D'Yvoire, R. Diament, M. Mariée, and J. Martin, *C. R. Acad. Sci.* **257,** 1094 (1963).
29. M. O'Keeffe and C. T. Perrino, *J. Phys. Chem. Solids* **28,** 211 (1967).
30. I. Olovsoon and P.-G. Jonsson, *in* "Hydrogen Bonding" (P. Schuster, G. Sundel, and C. Sandorfy, Eds.), Vol. II, Chap. 8. North Holland, Amsterdam, 1976.
31. M. Ichikawa, *Acta Crystallogr. B* **43,** 23 (1987).
32. M. Catti, G. Ferraris, and G. Ivaldi, *Acta Crystallogr. Sect. B* **35,** 525 (1979).
33. E. Kemnitz, C. Werner, and S. I. Trojanov, *Eur. J. Solid State Inorg. Chem.* **33**(6), 563 (1996).
34. F. Liebau, "Structural Chemistry of Silicates: Structure, Bonding, and Classification," p. 161. Springer-Verlag, Berlin, 1985.
35. K.-D. Kreuer, *Chem. Mater.* **8**(3), 610 (1996).
36. P. M. Calkins, M.S. Thesis, University of Washington, Seattle, 1996.
37. M. Ichikawa, T. Gustafsson, and I. J. Olovsson, *J. Mol. Structure* **321,** 21 (1994).